frontiers | Frontiers in Physics

ORIGINAL RESEARCH
published: 14 July 2022
doi: 10.3389/fphy.2022.859985

Facile Fabrication of Single-Layer Janus Membrane for Underwater Bubble Unidirectional Transport

Chunhua Liu[1], *Yun Peng*[1,2]*, *Conglin Huang*[1], *Jiaoping Shang*[2], *Guohua Liu*[1] *and Yibao Li*[1,2]*

[1]*Key Laboratory of Organo-pharmaceutical Chemistry of Jiangxi Province, Gannan Normal University, Ganzhou, China,*
[2]*Engineering Research Center of Jiangxi Province for Bamboo-based Advanced Materials and Biomass Conversion, Gannan Normal University, Ganzhou, China*

Janus membranes with superwetting play an important role in many fields, such as oil/water separation, unidirectional fluid transportation, microfluidic devices, intelligent ion valve, mass/heat transfer applications, etc. Although there has been some progress in the preparation of the Janus membranes with unidirectional penetration, it still remains a great difficulty for facile fabrication of two dimensional Janus membranes with a large pore structure and stable bubble unidirectional transport in the water. Herein, a signal-layer Janus membrane with superwetting is fabricated via the method of liquid-regulated hydrophobic modification strategy. The resultant Janus mesh achieves underwater unidirectional penetration. Namely, Underwater bubbles can pass unidirectionally from superhydrophobic side to hydrophilic side, but are blocked from passing through in the opposite direction. Thus, this Janus membrane with the unidirectional underwater bubbles penetration "diode" performance. We believe this work can promote the development of multi-dimensional Janus materials for fluid directional transport.

Keywords: bioinspired, Janus membrane, superhydophilicity, unidirectional transport, bubble

OPEN ACCESS

Edited by:
Malgorzata Biczysko,
Shanghai University, China

Reviewed by:
Yucai Lin,
Fujian Normal University, China
Chao Teng,
Qingdao University of Science and Technology, China

***Correspondence:**
Yun Peng
pengyun@buaa.edu.cn
Yibao Li
liyibao@gnnu.edu.cn

Specialty section:
This article was submitted to Physical Chemistry and Chemical Physics, a section of the journal Frontiers in Physics

Received: *22 January 2022*
Accepted: *03 May 2022*
Published: *14 July 2022*

Citation:
Liu C, Peng Y, Huang C, Shang J, Liu G and Li Y (2022) Facile Fabrication of Single-Layer Janus Membrane for Underwater Bubble Unidirectional Transport. Front. Phys. 10:859985. doi: 10.3389/fphy.2022.859985

INTRODUCTION

Membrane technology plays a significant role in modern separation technology and energy applications [1–5]. Particularly in the application of functional membrane with special wettability in oil-water separation [6–9], fog collection [10, 11], wastewater treatment [12, 13], catalytic contactor [14, 15], osmosis energy harvesting [16–18], aeration [19], and so on [20–23]. Janus membranes are a typical example, which exhibit asymmetric wettability, achieving manipulate liquid wetting and transport behavior by the aid of regulating the gas/liquid/solid multiphase interface [24, 25]. For example, Lin et al. prepared the fabrics with a unidirectional water-transfer effect by a special coating technique to construct a wettability gradient across the fabric thickness [26]. A Janus membrane aerator with superaerophobic-hydrophobic is fabricated by means of single-side polydopamine/polyethyleneimine codeposition, and it significantly promotes fine bubble generation and gas/liquid mass transfer [14]. A Janus copper foam with superhydrophobicity and superhydrophilicity by a novel method for on-demand oil/water separation is reported [27]. Cao et al. reported hydrophobic/hydrophilic cooperative Janus system that achieved reinforced fog collection ability by learning from nature's strategy [28]. Although the preparation method is simple and operation, but the interfacial stability is relatively weak. Recently, the bubble transport behavior at the superwetting interface has aroused great interest of researchers. Sun et al. constructed various electrodes of nanomaterials with superaerophobicity and applied in energy conversion [29–32].

Moreover, Jiang and co-workers carried out a series of studies about the behaviors of gas bubbles on solid interfaces, including generation, growth, coalescence, release, transport, and collection [33–37]. However, to date, there is still a challenge both simple preparation of single-layer Janus material and directional manipulation of the bubble, improve the practical application in the field of pipe transportation of fluid, corrosion of ocean vessels, and control of foaming process.

Herein, we adopted a water-controlled infiltration strategy to fabricate a single-layer copper mesh (CM) with superhydrophobic and hydrophilic to achieve underwater bubble unidirectional penetration, demonstrating a new underwater bubble "diode". We show that the bubble can penetrate through the Janus mesh from the superaerophobic side to the aerophilic side, but cannot penetrate from the other way around, owing to the competition of the bubble penetration and sprawl on the mesh. It is the cooperative driving forces of the gradient of Laplace pressure and ambient pressure that overcome the buoyant forces of bubbles to enable the desired unidirectional transport. This work demonstrates a promising methodology on guiding the mechanical behaviors of bubbles in water, which holds promise for applications in microfluidics or microdetectors.

EXPERIMENTAL SECTION

Materials

Commercial copper meshes (CMs) were supplied by Tairun Wire Mesh Co. Ltd., Hebei, China. Polydimethyl siloxane (PDMS) elastomer (containing pre-polymer and curing agent) was purchased from Dow Corning Corporation (Sylgard 184, United States). Ammonium persulfate was purchased from Xilong Chemical Co. Ltd., Beijing, China. 1H,1H,2H, 2H-Perfluorodecyl trimethoxysilane (97%, AR) was purchased from Aladdin, Hydrochloric acid, ethanol (95%, AR), sodium hydroxide, ammonium persulfate were purchased from Beijing Chemical Co. Ltd. All chemicals were used as received without further purification. Laboratory-made deionized water was used for all experiments and tests.

Fabrication of the Janus Copper Mesh

CMs were cleaned with ethanol to remove organic matter, then immersed in 1 M hydrochloric acid solution for 10 min to eliminate surface oxides, followed by rinsing with deionized water. Immerse the precleaned CMs in an alkaline erosion solution of 2.5 M NaOH and 0.15 M $(NH_4)_2S_2O_8$ for 8 min at room temperature. The underwater superhydrophilic/superaerophobic CMs were obtained after washing with deionized water and drying in the air. The PDMS pre-polymer was mixed with curing agents in the proportion of 10:1 (m/m), followed by manual stirring and vacuum degassing. Then, the homogeneous PDMS mixture was put in the oven at 60 °C for about 30 min. Afterward, the etched CM was placed on the surface of the pre-curing PDMS and thermal contacted for 10 s. And then, deionized water was added to the upper side of the etched CM to maintain the hydrophilicity. Moreover, hydrophobic side of the Janus CM was further modified with fluoroalkylsilane (FAS, $C_{10}H_4F_{17}Si(OCH_3)_3$ by vapor deposition. Finally, a series of underwater superhydrophobic/hydrophilic Janus CM were prepared.

Underwater Bubble Unidirectional Penetration Experiment

The Janus mesh with underwater superhydrophobic/hydrophilic is horizontally fixed in the middle of the square quartz tank filled with water by clips. The bubble of air was provided without a break by a Longer syringe pump (LSP01-1C, China) with a speed of 1 ml/h. To record the process of air bubble penetration using a digital camera.

Characterization and Instruments

The surface morphologies of the samples were characterized by field-emission scanning electron microscopy (JSM-7500F, Japan). All the contact angles of the CMs were measured with a contact angle analyzer (OCA 20, Data Physics, Germany). The optical images of the CM and the detailed process of underwater bubble unidirectional penetration experiments were recorded by a digital camera (Canon, Japan).

RESULTS AND DISCUSSION

As shown in **Figure 1**, the fabrication process of the single-layer Janus CM mainly consists of alkaline solution etching and FAS modification. Significantly, the critical step is water wetting-controlled modification. In the fabrication procedure of a single-layer Janus CM, to control the contact time between pre-curing PDMS and lower layer CM by means of adding deionized water. As the contact time is increased, the hydrophobic molecules of the PDMS pre-polymer continuously diffuse to the upper layer of the CM, resulting in the whole CM is superhydrophobicity. Therefore, the single-layer Janus CM can be prepared with water controlling the diffusion of hydrophobic molecules. Compared with the Janus membrane demonstrated in previous work,[9] the current Janus mesh possesses a smaller mesh thickness, which can heighten the flow rate, conducive to promoting underwater air bubble transportation.

A superhydrophilic mesh was prepared at room temperature by etching the CM in an alkaline corrosive solution consisting of NaOH and $(NH_4)_2S_2O_8$ (**Figure 1B**). For the original CM with a smooth surface, as shown in **Supplementary Figure S1**. After hydrophobic controllable modification, a hydrophilic/superhydrophobic Janus mesh was obtained (**Figure 1C**). SEM images and contact angles for both the superhydrophobic side and the hydrophilic side of the single-layer Janus CM as shown in **Figure 2**. Needle-like $Cu(OH)_2$ nanowires, with a diameter of 300–400 nm and length of 2.5–3.5 um (**Figures 2A,B**). Moreover, massive hydrophobic substances discontinuously cover the surface of needle-like $Cu(OH)_2$ nanowires, resulting in the wettability of the hydrophobic side of the Janus CM is enhanced. The water contact angle (WCA) is 151° ± 1.1°

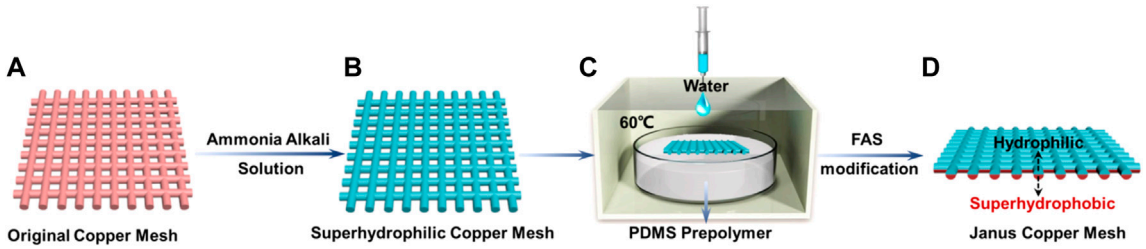

FIGURE 1 | The schematic of the fabrication procedure of single-layer Janus CM. **(A)** Pre-cleaned CM. **(B)** The etched CM with superhydrophobicity. **(C)** Single-layer modification of CM by a water wetting-controlled strategy. **(D)** A Janus CM with hydrophilic/superhydrophobic after FAS modification.

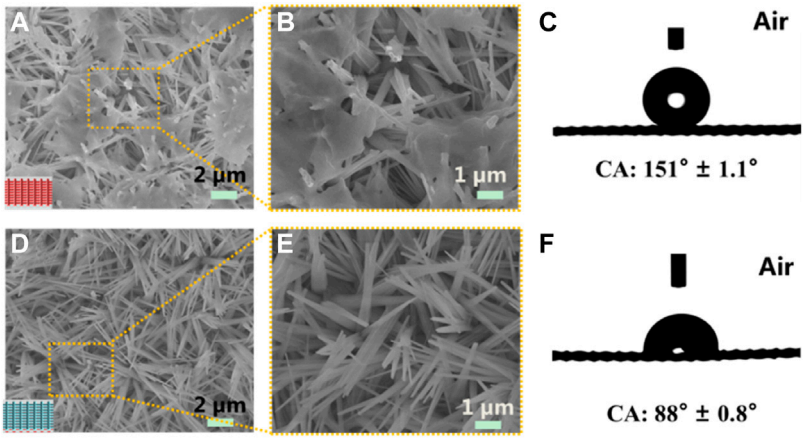

FIGURE 2 | The surface morphology and wettability of a single-layer Janus CM. **(A,B)** SEM images of the upper SHB side of the Janus CM. **(D,E)** SEM images of the lower HL side of the Janus CM. Contact angle images of the SHB side **(C)** and the HL **(F)** of the Janus CM in air, respectively.

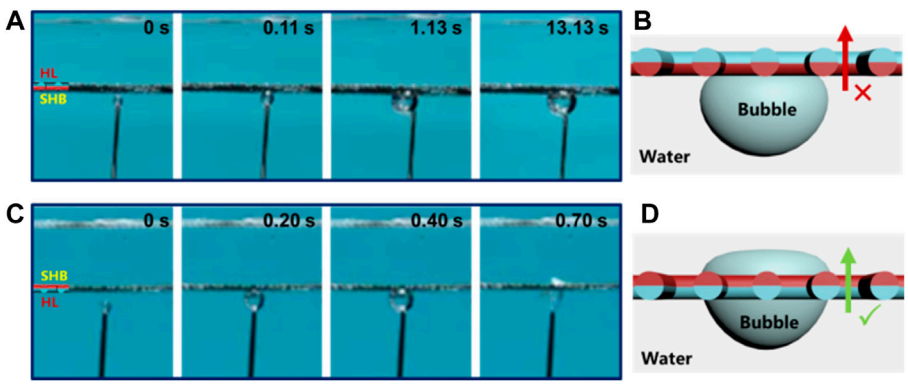

FIGURE 3 | Underwater bubble unidirectional penetration on the single-layer Janus CM fixed horizontally in the water. **(A)** Air bubbles will be blocked from the superhydrophobic side to the hydrophilic side. **(B)** As the superhydrophobic surface is fixed down, there is no Laplace pressure difference (P_L), the bubble cannot penetrate the single-layer Janus mesh. **(C)** Air bubbles can easily pass through the single-layer mesh from the hydrophilic side to superhydrophobic side. **(D)** As the hydrophilic surface is fixed down, the bubble can easily pass through the single-layer Janus mesh driven by the buoyant force (F_B) and Laplace pressure difference (P_L).

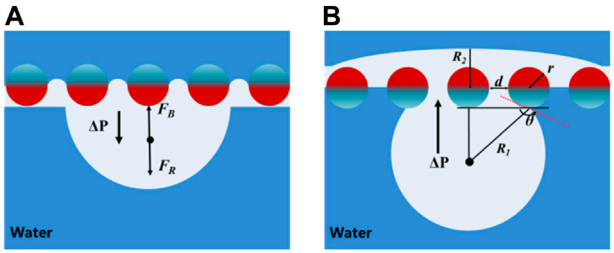

FIGURE 4 | Schematic diagram of underwater bubble unidirectional penetration on a single grid. **(A)** Air bubble cannot penetrate the superhydrophobic side but can sprawl. **(B)** Air bubble can penetrate the hydrophilic side and combine with the captured air layer on the superhydrophobic side surface.

(**Figure 2C**). In contrast, $Cu(OH)_2$ crystal is still distributed on the surface of the hydrophilic side of the Janus CM (**Figures 2D,E**), showing hydrophilic characteristics, and the WCA is 88° ± 0.8° (**Figure 2F**). As the resultant superhydrophobic/hydrophilic Janus CM is placed underwater, the superhydrophobic side is superaerophilic and the hydrophilic side is aerophobic. The superhydrophobic side of the Janus CM can catch an air layer on its surface, and serve as the superaerophilic layer for the underwater bubbles, while the hydrophilic side of the Janus CM can seize a water layer on its surface, and serve as the aerophobic layer for the underwater bubbles. Therefore, the single-layer Janus CM with superaerophilicity/aerophobicity is constructed through a liquid-regulated hydrophobic modification strategy.

As shown in **Figure 3**, the underwater bubble unidirectional transmission is further examined in conditions where we placed the single-layer Janus mesh horizontally in the water. The air bubble is blocked from the superhydrophobic side (**Figure 3A**). The small air bubble first contacts the superhydrophobic side of Janus mesh, in which an air layer is captured on the surface of the superhydrophobic side in the water. As the small air bubble approaches the superhydrophobic side, it merges with the trapped air layer and spreads out on the surface of superhydrophobic side, and thus the air bubble cannot pass through the single-layer Janus mesh. However, the superhydrophobic side is up and the hydrophilic side is down (**Figure 3C**), the air bubble passes through the hydrophilic side partly and touches the superhydrophobic side of the single-layer Janus mesh, achieving the penetration with driven force originating from the bubble buoyant force (F_B) and Laplace pressure difference (P_L). From the above experiments of the air bubble unidirectional penetration, it can be concluded that the single-layer Janus CM possesses the diode transport behavior.

As shown in **Figure 4**, a hypothetical mechanism is suggested to interpret the underwater air bubble unidirectional penetration phenomenon. The single-layer Janus CM is 60#, the diameter of a copper wire is 0.17 mm and the pore diameter is 253 μm. During the air bubble penetration experiment, the air layer on the superhydrophobic surface plays a decisive role. When the air bubble touches the hydrophilic side, the bubble is intercepted and failed to penetrate the Janus CM (**Figure 4A**). Because the superhydrophobic side (aerophilic side) is lower and the hydrophilic side (superhydrophobic side) is upper, resulting in a gas film on the lower superhydrophobic side interface. The air bubble first contacts the gas-film and fuses into the gas-film. In contrast, as the hydrophilic side is above and superhydrophobic side is below, the water enters micro/nano binding structure. Meanwhile, the air bubble upon touching the superhydrophobic side of single-layer Janus mesh can through the water layer caught in the gaps of the hydrophilic mesh grid, generating a gas channel between the bubble and the upper-gas layer. As a result, the air bubble firstly moves upward with the action of buoyancy and penetrates the water layer, then merges with the thin gas-film on the surface of the superhydrophobic side. Finally, with the continuous increase of bubble volume, the air bubble penetrates the Janus CM and separates from its surface resulting from the combined action of buoyancy force and Laplace pressure. In this process, buoyancy force and Laplace pressure are both upward forces, forming an upward resultant force. Interestingly, a differential Laplace pressure appears in the gas phase, in which the radius of curvature of the air bubble is importantly smaller than that of the upper superhydrophobic gas-layer. According to Young–Laplace **Equation 1**:

$$\Delta P = \gamma\left(\frac{1}{R_1} - \frac{1}{R_2}\right) \tag{1}$$

where γ is the surface tension of water, R_1 is the radius of curvature of the air bubble, R_2 is the radius of curvature of the gas-film, r is the diameter of a copper wire. Obviously, R_1 is smaller than R_2, so the Laplace pressure of the air bubble is greater than that in the lower layer.

Throughout the process, the buoyancy force (F_B) of air bubble plays a significant role in the process of bubble transmission across the water film, and the Laplace pressure difference plays another critical role in the penetration process when the bubble and the gas-film are combined [38–41]. Based on the above analysis, the minimum critical force (ΔP_{min}) of bubble penetration through the single-layer Janus CM can be calculated quantitatively. Suppose the bubble is a regular sphere with radius R_1, the bubble volume can be calculated according to the **Equations 2**, **3**:

$$V = \frac{4}{3}\pi R_1^3 \tag{2}$$

$$F_B = \rho g V \tag{3}$$

where V is the volume of air bubble, ρ is the density of water (1 g/cm^3), g is the gravity acceleration (9.8 m/s. In the experiment, the air bubble is subject to the resistance (F_R) of water, but the volume of the air bubble is about 250 μm, which the F_R may be negligible. After calculation, the driving force of 180 Pa can be generated by the Laplace pressure, while the driving force caused by the buoyancy of the bubble itself is only 1.6×10^{-10} Pa, the former is far greater than the latter. Therefore, the bubble moves vertically upward only under the force of Laplace pressure. Moreover, a critical pressure to penetrate the CM when the small air bubble is transmitted upward through Janus copper also can be calculated by the **Equations 4**, **5**:

$$P = \frac{4\gamma|\cos\theta|}{4} \quad (4)$$

$$D = 2r + d \quad (5)$$

where θ is the contact angle of underwater bubbles, d is the mesh aperture, and D is the width of bubbles passing through CM. In this work, the diameter of a copper wire is 0.17 mm and the pore diameter is 253 μm. According to **Eqs. 4**, **5**, the critical penetration pressure is 420 Pa. Therefore, the difference of Laplace pressure (P_L) should cause the movement of air bubbles toward the upper layer of superhydrophobic side.

Significantly, the parameter of pore size plays a crucial role in water permeation[14] Next, we further explore how the pore size of our meshes affects the unidirectional penetration. According to **Eqs 4**, **5**, we calculated 20#, 40#, 80#, and 100# CM, respectively (**Supplementary Figure S2**). The results show that the critical penetration pressure increases with the increase of the mesh number of CM (**Supplementary Table S1**). In other words, the smaller of pore size of the single-layer Janus CM, the greater the resistance of air bubbles through CM. The theoretical results are consistent with the experimental results.

CONCLUSION

In summary, a novel method was reported for the preparation of the single-layer Janus CMs. Based on the Janus CM with superhydrophobicity and hydrophilicity, we realize the underwater air bubble unidirectional transportation. The experimental results show that the bubble can easily pass through the Janus mesh from the hydrophilic side to superhydrophobic side, while it is blocked from the superhydrophobic side to hydrophilic side, due to the competition of the air bubble penetration and spread on the mesh surface with special infiltrating. This interestingly enables an underwater bubble "diode". The transporting behavior of underwater bubbles is controllably regulated by surface infiltrating and pore size of the Janus mesh. This work presents a facile method to fabricate a single-layer mesh gas diode Janus membrane, and may serve as enlightening clues for the design and preparation of smart materials and new technologies for practical applications in fluid transportation pipes, engineering vessels, and froth flotation processes.

DATA AVAILABILITY STATEMENT

The original contributions presented in the study are included in the article/**Supplementary Material**, further inquiries can be directed to the corresponding authors.

AUTHOR CONTRIBUTIONS

YP: Design and guide experiment; CL: Article writing and revision; YL:Theoretical direction; CH: Experimental operation and data collection; JS: Experimental data collection and analysis; GL: Experimental operation and data collection.

FUNDING

This work was supported by the National Natural Science Foundation of China (No.21902033), the Jiangxi Province Youth Science Foundation Project (No. 20192BAB216013, 20202BABL214057), the Science and Technology Project of Jiangxi Province Education Department (No. 180775), 2020 National Innovation and Entrepreneurship Training Program for College Students No.202010418007.

SUPPLEMENTARY MATERIAL

The Supplementary Material for this article can be found online at: https://www.frontiersin.org/articles/10.3389/fphy.2022.859985/full#supplementary-material

REFERENCES

1. Logan BE, Elimelech M, Membrane-based Processes for Sustainable Power Generation Using Water. *Nature* (2012) 488:313–9. doi:10.1038/nature11477
2. Werber JR, Osuji CO, Elimelech M, Materials for Next-Generation Desalination and Water Purification Membranes. *Nat Rev Mater* (2016) 1: 16018. doi:10.1038/natrevmats.2016.18
3. Lee A, Elam JW, Darling SB, Membrane Materials for Water Purification: Design, Development, and Application. *Environ Sci Water Res Technol* (2016) 2:17–42. doi:10.1039/c5ew00159e
4. Jain H, Garg MC, Fabrication of Polymeric Nanocomposite Forward Osmosis Membranes for Water Desalination-A Review. *Environ Tech Innovation* (2021) 23:101561. doi:10.1016/j.eti.2021.101561
5. Wang J, Ma X, Zhou J, Du F, Teng C, Bioinspired, High-Strength, and Flexible MXene/Aramid Fiber for Electromagnetic Interference Shielding Papers with Joule Heating Performance. *ACS Nano* (2022) 16:6700–11. doi:10.1021/acsnano.2c01323
6. Ismail NH, Salleh W, Ismail AF, Hasbullah H, Jaafar J, Hydrophilic Polymer-Based Membrane for Oily Wastewater Treatment: A Review. *Sep.Purif Technol* (2019) 233:116007.
7. Bolto B, Zhang J, Wu X, Xie Z, A Review on Current Development of Membranes for Oil Removal from Wastewaters. *Membranes* (2020) 10:65. doi:10.3390/membranes10040065
8. Zhang JC, Liu L, Si Y, Yu JY, Ding B, Electrospun Nanofibrous Membranes: An Effective Arsenal for the Purification of Emulsified Oily Wastewater. *Adv Funct Mater* (2020) 30:2002192. doi:10.1002/adfm.202002192
9. Zhang W, Qu R, Li X, Liu Y, Wei Y, Feng L, A Dual Functional Janus Membrane Combining Superwettability with Electrostatic Force for Controllable Anionic/cationic Emulsion Separation and *In Situ* Surfactant Removal. *J Mater Chem A* (2019) 7:27156–63. doi:10.1039/c9ta10390b
10. Ding Y, Tu K, Burgert I, Keplinger T, Janus wood Membranes for Autonomous Water Transport and Fog Collection. *J Mater Chem A* (2020) 8:22001–8. doi:10.1039/d0ta07544b
11. Ren F, Li G, Zhang Z, Zhang X, Fan H, Zhou C, et al. A Single-Layer Janus Membrane with Dual Gradient Conical Micropore Arrays for Self-Driving Fog Collection. *J Mater Chem A* (2017) 5:18403–8. doi:10.1039/c7ta04392a

12. Ahmad KF, Gordon MK, Anita B, Huda AS, Filip M, Marwan K, et al. Inorganic Membranes: Preparation and Application for Water Treatment and Desalination. *Materials* (2018) 11:74.
13. Wang P, Wang Z, Wu Z, Mai S, Fouling Behaviours of Two Membranes in a Submerged Membrane Bioreactor for Municipal Wastewater Treatment. *J Membr Sci* (2011) 382:60–9. doi:10.1016/j.memsci.2011.07.044
14. Yang H-C, Hou J, Wan L-S, Chen V, Xu Z-K, Janus Membranes with Asymmetric Wettability for Fine Bubble Aeration. *Adv Mater Inter* (2016) 3:1500774. doi:10.1002/admi.201500774
15. Li C, Pi Y, Liu S, Feng J, Zhang X, Li S, et al. Phosphotungstate-Functionalized Mesoporous Janus Silica Nanosheets for Reaction-Controlled Pickering Interfacial Catalysis. *ACS Sustain Chem. Eng.* (2021) 9:13501–13. doi:10.1021/acssuschemeng.1c04418
16. Ma TJ, Balanzat E, Janot JM, Balme S, Nanopore Functionalized by Highly Charged Hydrogels for Osmotic Energy Harvesting. *ACS Appl Mater Inter* (2019) 11:12578–85. doi:10.1021/acsami.9b01768
17. Pakulski D, Czepa W, Buffa SD, Ciesielski A, Samorì P, Atom-Thick Membranes for Water Purification and Blue Energy Harvesting. *Adv Funct Mater* (2020) 30:1902394. doi:10.1002/adfm.201902394
18. Zhou S, Xiong X, Liu L, Lin H, Wang J, Li T, et al. Novel Janus Membrane with Unprecedented Osmosis Transport Performance. *J Mater Chem A* (2019) 7: 632–8. doi:10.1039/c8ta08541b
19. Ibrahim R, Zainon Noor Z, Baharuddin N, Ahmad Mutamim N, Yuniarto A, Microbial Fuel Cell Membrane Bioreactor in Wastewater Treatment, Electricity Generation and Fouling Mitigation. *Chem Eng Technol* (2020) 43:1908–21. doi:10.1002/ceat.202000067
20. Xiao H, Wu H, Zhang X, Wei C, Chen D, Huang X, The Micro-volume Liquid Focusing Effect in Janus Membrane and its Biosensing Application. *J Colloid Interf Sci.* (2021) 592:22–32.
21. Zhou Q, Li H, Li D, Wang B, Wang G, Bai J, et al. A Graphene Assembled Porous Fiber-Based Janus Membrane for Highly Effective Solar Steam Generation. *J Colloid Interf Sci* (2021) 592:77–86. doi:10.1016/j.jcis.2021.02.045
22. Lv Y, Li Q, Hou Y, Wang B, Zhang T, Facile Preparation of an Asymmetric Wettability Janus Cellulose Membrane for Switchable Emulsions' Separation and Antibacterial Property. *ACS Sustain Chem. Eng.* (2019) 7:15002–11. doi:10.1021/acssuschemeng.9b03450
23. Yong J, Yang Q, Hou X, Chen F, Emerging Separation Applications of Surface Superwettability. *Nanomaterials* (2022) 12:688. doi:10.3390/nano12040688
24. Yang H-C, Xie Y, Hou J, Cheetham AK, Chen V, Darling SB, Janus Membranes: Creating Asymmetry for Energy Efficiency. *Adv Mater* (2018) 30:1801495. doi:10.1002/adma.201801495
25. Wang Z, Li H, Yang X, Guan M, Wang L, Multi-Bioinspired Janus Copper Mesh for Improved Gravity-Irrelevant Directional Water Droplet and Flow Transport. *Langmuir* (2022) 38:2137–44. doi:10.1021/acs.langmuir.1c03267
26. Wang H, Ding J, Dai L, Wang X, Lin T, Directional Water-Transfer through Fabrics Induced by Asymmetric Wettability. *J Mater Chem* (2010) 20:7938–40. doi:10.1039/c0jm02364g
27. Liu C, Peng Y, Huang C, Ning Y, Shang J, Li Y, Bioinspired Superhydrophobic/Superhydrophilic Janus Copper Foam for On-Demand Oil/Water Separation. *ACS Appl Mater Inter* (2022) 14:11981–8. doi:10.1021/acsami.2c00585
28. Cao M, Xiao J, Yu C, Li K, Jiang L, Hydrophobic/Hydrophilic Cooperative Janus System for Enhancement of Fog Collection. *Small* (2015) 11:4379–84. doi:10.1002/smll.201500647
29. Han N, Yang KR, Lu Z, Li Y, Xu X, Gao T, et al. Nitrogen-doped Tungsten Carbide Nanoarray as an Efficient Bifunctional Electrocatalyst for Water Splitting in Acid. *Nat Commun* (2018) 9:924. doi:10.1038/s41467-018-03429-z
30. Kuang Y, Kenney MJ, Meng Y, Hung WH, Liu Y, Huang JE, et al. Solar-driven, Highly Sustained Splitting of Seawater into Hydrogen and Oxygen Fuels. *Proc Natl Acad Sci U S A* (2019) 116:6624–9. doi:10.1073/pnas.1900556116
31. Zhong Y, Xu Y, Ma J, Wang C, Sheng S, Cheng C, et al. An Artificial Electrode/Electrolyte Interface for CO 2 Electroreduction by Cation Surfactant Self-Assembly. *Angew Chem Int Ed* (2020) 59:19095–101. doi:10.1002/anie.202005522
32. Lu Z, Sun M, Xu T, Li Y, Xu W, Chang Z, et al. Superaerophobic Electrodes for Direct Hydrazine Fuel Cells. *Adv Mater* (2015) 27:2361–6. doi:10.1002/adma.201500064
33. Yu C, Zhang P, Wang J, Jiang L, Superwettability of Gas Bubbles and its Application: From Bioinspiration to Advanced Materials. *Adv Mater* (2017) 29:1703053. doi:10.1002/adma.201703053
34. Zhang C, Zhang B, Ma H, Li Z, Xiao X, Zhang Y, et al. Bioinspired Pressure-Tolerant Asymmetric Slippery Surface for Continuous Self-Transport of Gas Bubbles in Aqueous Environment. *ACS Nano* (2018) 12:2048–55. doi:10.1021/acsnano.8b00192
35. Yu C, Cao M, Dong Z, Li K, Yu C, Wang J, et al. Aerophilic Electrode with Cone Shape for Continuous Generation and Efficient Collection of H2Bubbles. *Adv Funct Mater* (2016) 26:6830–5. doi:10.1002/adfm.201601960
36. Li W, Zhang J, Xue Z, Wang J, Jiang L, Spontaneous and Directional Bubble Transport on Porous Copper Wires with Complex Shapes in Aqueous Media. *ACS Appl Mater Inter* (2018) 10:3076–81. doi:10.1021/acsami.7b15681
37. Chen J, Liu Y, Guo D, Cao M, Jiang L, Under-water Unidirectional Air Penetration via a Janus Mesh. *Chem Commun* (2015) 51:11872–5. doi:10.1039/c5cc03804a
38. Feng L, Li S, Li Y, Li H, Zhang L, Zhai J, et al. Super-Hydrophobic Surfaces: From Natural to Artificial. *Adv Mater* (2002) 14:1857–60. doi:10.1002/adma.200290020
39. Zhang H, Hao H, Jackson JK, Chiao C, Yu H, Janus Ultrathin Film from Multi-Level Self-Assembly at Air-Water Interfaces. *Chem Commun* (2014) 50: 14843–6. doi:10.1039/c4cc06798c
40. Liu K, Cao M, Fujishima A, Jiang L, Bio-Inspired Titanium Dioxide Materials with Special Wettability and Their Applications. *Chem Rev* (2014) 114: 10044–94. doi:10.1021/cr4006796
41. Pei C, Peng Y, Zhang Y, Tian D, Liu K, Jiang L, An Integrated Janus Mesh: Underwater Bubble Antibuoyancy Unidirectional Penetration. *ACS Nano* (2018) 12:5489–94. doi:10.1021/acsnano.8b01001

Conflict of Interest: The authors declare that the research was conducted in the absence of any commercial or financial relationships that could be construed as a potential conflict of interest.

Publisher's Note: All claims expressed in this article are solely those of the authors and do not necessarily represent those of their affiliated organizations, or those of the publisher, the editors and the reviewers. Any product that may be evaluated in this article, or claim that may be made by its manufacturer, is not guaranteed or endorsed by the publisher.